

LETTERS

Molecular robots guided by prescriptive landscapes

Kyle Lund^{1,2}, Anthony J. Manzo³, Nadine Dabby⁴, Nicole Michelotti^{3,5}, Alexander Johnson-Buck³, Jeanette Nangreave^{1,2}, Steven Taylor⁶, Renjun Pei⁶, Milan N. Stojanovic^{6,7}, Nils G. Walter³, Erik Winfree^{4,8,9} & Hao Yan^{1,2}

Traditional robots¹ rely for their function on computing, to store internal representations of their goals and environment and to coordinate sensing and any actuation of components required in response. Moving robotics to the single-molecule level is possible in principle, but requires facing the limited ability of individual molecules to store complex information and programs. One strategy to overcome this problem is to use systems that can obtain complex behaviour from the interaction of simple robots with their environment^{2–4}. A first step in this direction was the development of DNA walkers⁵, which have developed from being non-autonomous^{6,7} to being capable of directed but brief motion on one-dimensional tracks^{8–11}. Here we demonstrate that previously developed random walkers¹²—so-called molecular spiders that comprise a streptavidin molecule as an inert ‘body’ and three deoxyribozymes as catalytic ‘legs’—show elementary robotic behaviour when interacting with a precisely defined environment. Single-molecule microscopy observations confirm that such walkers achieve directional movement by sensing and modifying tracks of substrate molecules laid out on a two-dimensional DNA origami

landscape¹³. When using appropriately designed DNA origami, the molecular spiders autonomously carry out sequences of actions such as ‘start’, ‘follow’, ‘turn’ and ‘stop’. We anticipate that this strategy will result in more complex robotic behaviour at the molecular level if additional control mechanisms are incorporated. One example might be interactions between multiple molecular robots leading to collective behaviour^{14,15}; another might be the ability to read and transform secondary cues on the DNA origami landscape as a means of implementing Turing-universal algorithmic behaviour^{2,16,17}.

We previously described polycatalytic assemblies, comprising streptavidin molecules and several attached nucleic-acid catalysts, that function as walkers and are referred to as molecular spiders¹². The molecular spiders used in this study comprise one streptavidin molecule as an inert body and three catalytic legs. The legs are adapted from the 8-17 DNA enzyme, which binds and cleaves oligodeoxynucleotide (henceforth ‘oligonucleotide’) substrates with a single ribose moiety (Fig. 1a, b) into two shorter products that have lower affinities for the enzyme¹⁸. The different substrate and product affinities ensure that a spider’s interactions with a layer of immobilized substrate and/or

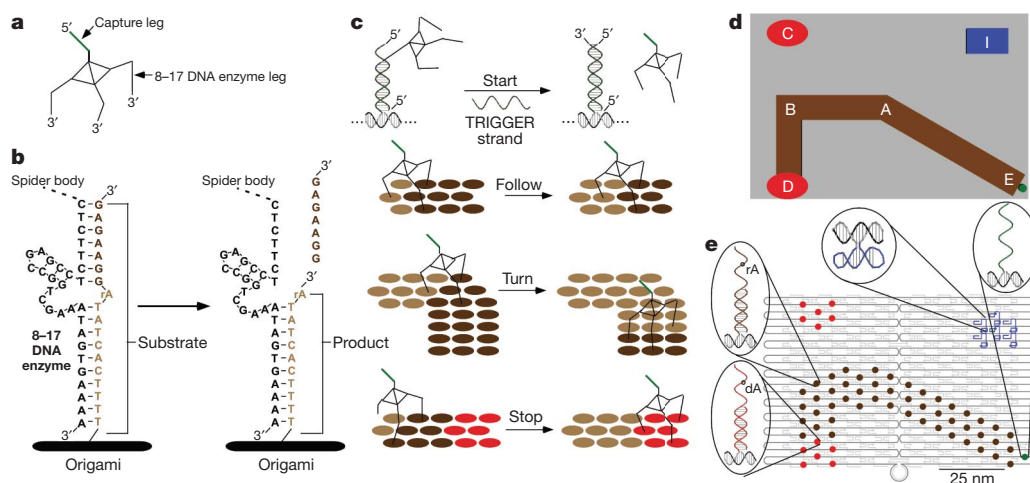


Figure 1 | Deoxyribozyme-based molecular walker and origami prescriptive landscape. **a**, The NICK3.4A₃₊₁ spider consists of a streptavidin core, with a 20-base single-stranded DNA (green) that positions the spider at the start, and three deoxyribozyme legs. **b**, The 8-17 deoxyribozyme cleaves its substrate at an RNA base, creating two shorter products (respectively 7 and 11 bases in length). Dissociation from these products allows legs to associate with the next substrate. **c**, Spider actions: after release by a 27-base single-stranded DNA trigger, the spider follows the

substrate track, turns and continues to a STOP site (red). **d**, Schematic of the DNA origami landscape with positions A–E labelled; track EABD is shown with I indicating a topographical imaging marker. **e**, A representative origami landscape showing the START position (green), the substrate track (brown), STOP and CONTROL sites (red), and a topographical imaging marker (blue). rA, ribonucleotide position at which cleavage occurs; dA, deoxyribonucleotide within non-chimeric and non-cleavable analogue of substrate at a STOP position.

¹Department of Chemistry and Biochemistry, Arizona State University, Tempe, Arizona 85287, USA. ²The Bidesign Institute, Arizona State University, Tempe, Arizona 85287, USA. ³Department of Chemistry, Single Molecule Analysis Group, University of Michigan, Ann Arbor, Michigan 48109, USA. ⁴Computation & Neural Systems, California Institute of Technology, Pasadena, California 91125, USA. ⁵Department of Physics, University of Michigan, Ann Arbor, Michigan 48109, USA. ⁶Division of Experimental Therapeutics, Department of Medicine, Columbia University, New York, New York 10032, USA. ⁷Department of Biomedical Engineering, Columbia University, New York, New York 10032, USA. ⁸Computer Science, California Institute of Technology, Pasadena, California 91125, USA. ⁹Bioengineering, California Institute of Technology, Pasadena, California 91125, USA.

product sites can be modelled using a simple ‘memory’ principle¹⁹: each leg moves independently from one site to an accessible neighbouring site, but if a leg is on a site not visited before, it will stay longer on average. Put biochemically, a deoxyribozyme attached to a site that was previously converted to a product will dissociate faster, whereas it will stick longer to substrates and will eventually cleave them. Because spiders have multiple legs that hinder complete dissociation, a single dissociated leg will quickly reattach to a nearby product or substrate site. After cleaving, each leg will thus explore neighbouring sites until it finds another substrate to bind to for longer. This ensures that the body of a spider positioned at the interface between products and substrates will move towards the substrate region, and that it will move directionally along a linear track as the substrates are cleaved. Previously engineered walkers using ‘burnt bridge’ mechanisms^{6–9,11} and Brownian ratchets found in nature²⁰ render revisiting the same path impossible, but our spiders will perform random Brownian walks on product sites until they again encounter a substrate track.

In analogy to the reactive planning used in simple robots⁴, the sensor–actuator feedback afforded when legs sense and modify nearby oligonucleotides allows us to design prescriptive landscapes that direct the spiders’ motion along a predefined path (Fig. 1c, d). Prescriptive landscapes were constructed using the DNA origami scaffolding technique¹³. The scaffold consists of a 7,249-nucleotide single-stranded DNA folded using 202 distinct staple strands into a rectangular shape roughly 65 nm × 90 nm × 2 nm in size and with 6-nm feature resolution (Fig. 1e). Each staple can be extended at its 5′ end with probes that recruit substrates, products, and goal and control DNA strands²¹.

We designed pseudo-one-dimensional tracks on origami of about the width of a molecular spider (three adjacent rows of substrates; Fig. 1d). Tracks are coded using a sequence of points, A, B, C, D and E, such that on an ABD landscape the spider starts at A and passes through B before ending at D. Staples were modified to position a START oligonucleotide—used to place a spider at the start of the experiment—that is complementary to a TRIGGER oligonucleotide used to release the spider²² (the ‘start’ action); substrate TRACK probes to capture the 5′ extension on substrates forming the TRACK (directing the ‘follow’ and ‘turn’ actions); STOP probes, complementary to the 5′ extension on STOP strands (non-chimeric and uncleavable analogues of the substrate) that do not influence directional movement but trap spiders to prevent them from walking backwards after completing the track (the ‘stop’ action); CONTROL probes (identical to STOP probes, but disconnected from the track), used to assess the extent to which free-floating spiders are captured directly from solution; and MARKER oligonucleotides based on inert dumb-bell hairpins, aiding in origami classification within atomic force microscopy (AFM) images (Fig. 1e). To position spiders at START sites, we replaced one of the four catalytic legs of the NICK-4.4A¹² spider with a tethering oligonucleotide (Supplementary Figs 1–4 and Supplementary Information) partly complementary to the START oligonucleotide.

To estimate the efficiency of spider motion directed by the TRACK, we defined and tested four paths with no (EAC), one (ABD), or two (EABD, EABC) turns (Fig. 2 and Supplementary Figs 8, 11, 14 and 17). The basic experimental procedure involves assembling the origami; attaching spiders to START sites; adding TRACK, STOP and CONTROL strands to complete the landscape; and initiating an experiment by releasing spiders through addition of TRIGGER and 1 mM Zn²⁺ cofactor²³ (Supplementary Figs 6 and 25 and Supplementary Information). We sampled the origami solution before and after spider release, and imaged individual samples by AFM to determine the locations of spiders. We scored only ‘face-up’ origami (substrates projected away from mica) to avoid artefacts, using procedures that minimize read-out bias (see Supplementary Information for details).

In all samples imaged before spider release, 30–40% of the assembled origami carried at least one spider, 80–95% of this origami were singly occupied, and in 80–90% of the singly occupied origami

the spider was bound at the START position (Supplementary Table 1 and Supplementary Figs 9, 10, 12, 13, 15, 16, 18 and 19). On adding TRIGGER, all four landscapes with substrate tracks showed that the fraction of spiders at the START diminishes with a concomitant increase in spiders observed on the STOP sites (Fig. 2c, g and Supplementary Fig. 23). A spider’s ability to reach the STOP sites decreased with increased TRACK length and with decreased time of incubation in solution. In time-lapse experiments on a long path (EABD, spanning ~90 nm) we observed a gradual increase of up to 70% in the proportion of spiders on STOP sites within 60 min (Fig. 2c, g). A short path (ABD, ~48 nm) was completed to the same extent within 30 min.

We captured a series of AFM images of a spider moving along an origami track (Fig. 3). The rate of spider movement (~90 nm over 30 min, with approximately 6 nm per three parallel cleavage events) was consistent with the processive cleavage rates (~1 min⁻¹) of spiders on a two-dimensional surface as obtained by surface plasmon resonance (SPR; Supplementary Fig. 6). More systematic sequential imaging proved difficult owing to mica’s inhibitory effects on the spider.

To confirm that spiders can indeed traverse product tracks by means of unbiased random walks, we tested spiders using EABD origami in which the substrate was replaced by product on the TRACK. Spiders still reached the STOP sites, albeit more slowly (Fig. 2f, g), as expected from purely Brownian spider movement even if individual steps are somewhat faster¹⁹.

If all three legs simultaneously dissociate before any leg reattaches, a spider could ‘jump’ by completely dissociating from the origami and subsequently reattaching elsewhere at random. Evidence against frequent jumping (or an excess of spiders in solution during the initial assembly stage) comes from the low level of spider occupancy at CONTROL sites in both substrate- and product-track experiments (Fig. 2c, e, g) and the stable proportions of unoccupied and multiply occupied origami (Supplementary Table 1; both before and after the addition of TRIGGER, 5–10% of origami had more than one spider on their track). In contrast, when spiders were released on ABD landscapes with no TRACK strands, after 30 min we observed an equal distribution between STOP and CONTROL sites (Supplementary Fig. 24 and Supplementary Table 2), as expected for a process that involves spider dissociation from, and random rebinding to, the origami.

In independent ensemble experiments using SPR to monitor spider attachment and with a constant flow passing over the surface, up to 15% of spiders dissociated from a non-origami, two-dimensional, product-covered surface within 60 min (Supplementary Fig. 5). When using similar surfaces but covered with substrate, spiders showed an average processivity of ~200 substrate sites before being removed by flow (Supplementary Figs 5 and 6). Together, the results of our control experiments rule out that spiders move predominantly by jumping; there is insufficient jumping even on product tracks to explain the 50–70% occupation of the STOP sites after walks on ABD, EABC and EABD substrate tracks.

To observe the movement of individual spiders in real time, we applied particle tracking by super-resolution total-internal-reflection fluorescence video microscopy²⁴. Four biotin molecules were attached to the underside of the origami for immobilization on the avidin-coated quartz slide. Spiders were covalently labelled with on average 2.3 Cy3 fluorophores, and STOP sites were labelled with 6 Cy5 fluorophores. The labelling allowed us to monitor changes in spider position relative to the STOP site by two-colour fluorescent particle tracking^{25,26}. In a typical experiment, spider-loaded tracks were incubated with TRIGGER and immobilized on the slide (Supplementary Fig. 26), and then Zn²⁺ was added to promote spider movement by means of substrate cleavage. Recognizing that the activity of 8-17 DNA enzyme depends on buffer conditions²³, we obtained the best results from SSC or HEPES with increased Zn²⁺ concentrations but without Mg²⁺ (Supplementary Figs 6 and 25).

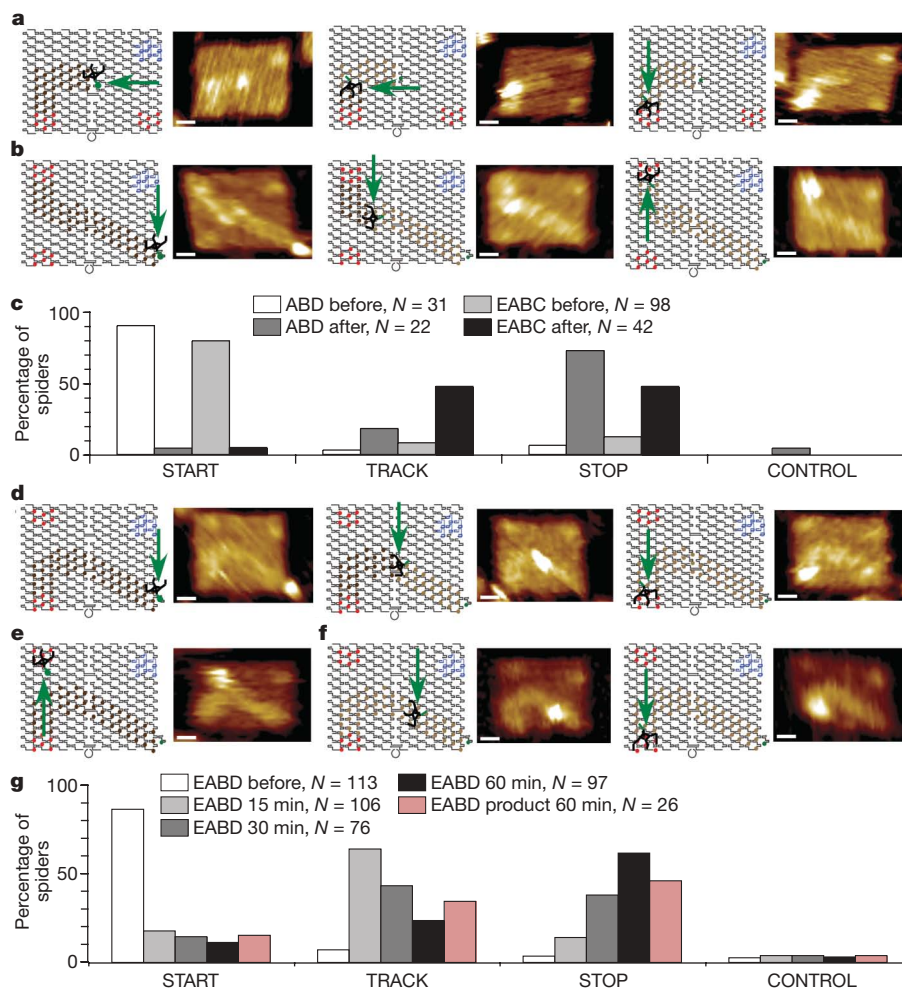


Figure 2 | Spider movement along three tracks and AFM images of the spider at the START, on the TRACK and at the STOP site. a, ABD track. b, EABC track. c, ABD and EABC spider statistics before and 30 min after release. d, EABD track. e, EABD track with spider on control. f, EABD

product-only track. g, EABD spider statistics before and 15, 30 and 60 min after release, and 60 min after release on the product-only track. All AFM images are $144 \text{ nm} \times 99.7 \text{ nm}$ and the scale bars are 20 nm. N , number of origami with a single spider that were counted for the given sample.

Our resolution was not sufficient to detect turns reliably, so we focused on EAC landscapes. Individual particle traces showed a distribution of behaviours that may result from variations across molecules, idiosyncrasies of the sample preparation, the stochastic nature of the observed process, photobleaching and/or instrument measurement error (Fig. 4a, b, Supplementary Figs 29–31, Supplementary Information and Supplementary Table 3). Despite this variability, traces of moving particles commonly showed net displacements of between 60 and 140 nm and mean speeds of between 1 and 6 nm min^{-1} ; within

error, these values are consistent with the track length ($\sim 90 \text{ nm}$) and the deoxyribozyme cleavage rate ($\sim 1 \text{ min}^{-1}$ per leg), respectively.

Tests with and without Zn^{2+} and/or TRIGGER, both on substrate and product tracks, yielded root mean squared (r.m.s.) displacement plots of the particle traces that in each case varied as expected on the basis of the behaviour of spiders on origami tracks, despite the inherent noise associated with single-particle tracking over tens-of-nanometre length scales and tens-of-minute time scales (Fig. 4c, d). For instance, r.m.s. displacement plots indicated substantially more movement on

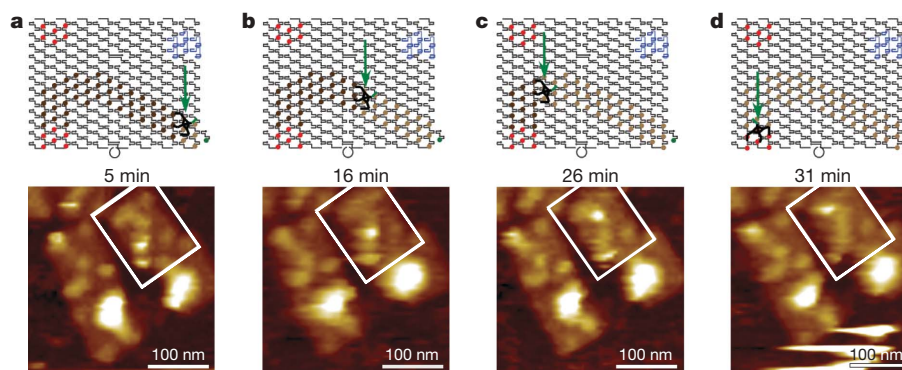


Figure 3 | AFM movie of spider movement. a–d, Schematics and AFM images of the spider moving along the EABD track 5 min (a), 16 min (b), 26 min (c) and 31 min (d) after TRIGGER was added. AFM images are $300 \text{ nm} \times 300 \text{ nm}$ and the scale bars are 100 nm.

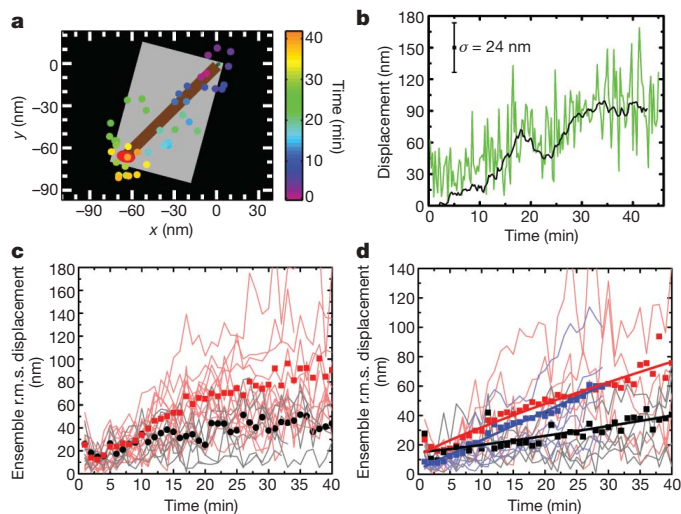


Figure 4 | Spiders imaged on origami tracks in real time using super-resolution total-internal-reflection fluorescence microscopy.

a, Position–time trajectory of a selected spider (EAC 2, Cy3-labelled) on the EAC substrate track. The position as a function of time is represented by colour-coded dots (see Supplementary Information for details). A small green dot (upper right) represents the START site and a large red oval (lower left) represents the Cy5-labelled STOP site. ZnSO_4 was added at time zero. **b**, Displacement of the spider trajectory in panel **a** from its initial position as a function of time. The green line represents displacement calculated from raw position measurements, and the black line represents the displacement calculated from a rolling 4-min average (Supplementary Information). σ , standard error of the mean of the raw displacement with respect to 4-min time bins. **c**, Ensemble r.m.s. displacement of exemplary spiders on the EAC substrate track in the presence (red, corresponding to the 15 Tier 1 Spiders in Supplementary Fig. 29) and absence (black, 7 spiders) of Zn^{2+} , with the corresponding displacements used to calculate each ensemble r.m.s. displacement for each buffer condition (similarly coloured line graphs). **d**, Ensemble r.m.s. displacement of spiders on EAC tracks satisfying simple filtering criteria. Curves are shown for spiders on the EAC substrate track (red, 85 spiders), the EAC product track with TRIGGER introduced to the sample 10–15 min before imaging (blue, 18 spiders) and the EAC product track with TRIGGER introduced 30–60 min before imaging (black, 29 spiders). The first two plots are fitted with a power-law function and the third is fitted with a straight line. Individual displacements are shown with colours corresponding to the respective ensemble r.m.s. displacement plots. All data were obtained in SSC buffer.

substrate tracks in the presence of Zn^{2+} and TRIGGER than in their individual absences (Fig. 4c, Supplementary Figs 30–32 and Supplementary Table 4). On product tracks, results were consistent with an unbiased random walk, independent of the presence of Zn^{2+} . When product tracks were pre-incubated with TRIGGER 30–60 min before addition of Zn^{2+} and the onset of imaging (as were substrate tracks), little or no movement was observed (Fig. 4d), consistent with spiders having been released and moving towards or reaching the STOP sites before imaging. In contrast, when TRIGGER and Zn^{2+} were both added shortly before imaging, substantial movement was observed (Fig. 4d), consistent with our AFM results for spiders on product tracks (Fig. 2f, g) and with Monte Carlo simulations of spider movement (Supplementary Information and Supplementary Fig. 32).

The results of our single-molecule experiments are consistent with DNA-based random walkers guided by their landscapes over distances as great as 100 nm, for up to 50 cleavage steps, at speeds of roughly 3 nm min^{-1} . We note, however, that the distance over which a spider can move is limited by dissociation and backtracking, and any increase in processivity comes at the cost of a lower speed¹². Other limitations arise from the mechanism consuming substrate that must be recharged to sustain directed movement, and from spiders being subject to the stochastic uncertainty as to whether each one can accomplish its task (compare with the notions of ‘faulty’ behaviour in robotics and ‘yield’ in chemistry). Furthermore, in comparison with protein-based walkers

using solution phase fuels²⁷, our walkers are not as fast, efficient or powerful. As candidates for molecular robots, however, they offer the advantages of programmability^{5,10,28–30}, predictable biophysical behaviour⁵ and interaction with designable landscapes¹³. The ability to obtain programmed behaviour from the interaction of simple molecular robots with a complex and adjustable environment suggests that by using stochastic local rules and programming the environment, we can effectively circumvent the limitations that molecular construction places on the complexity of robotic behaviour at the nanoscale.

Received 31 March 2009; accepted 11 March 2010.

1. Siegwart, R. & Nourbakhsh, I. R. *Introduction to Autonomous Mobile Robots* (MIT Press, 2004).
2. Turing, A. M. On computable numbers, with an application to the Entscheidungsproblem. *Proc. London Math. Soc.* **42**, 230–265 (1936).
3. Braitenberg, V. *Vehicles: Experiments in Synthetic Psychology* (MIT Press, 1984).
4. Brooks, R. A. Intelligence without representation. *Artif. Intell.* **47**, 139–159 (1991).
5. Bath, J. & Turberfield, A. J. DNA nanomachines. *Nature Nanotechnol.* **2**, 275–284 (2007).
6. Sherman, W. B. & Seeman, N. C. A precisely controlled DNA biped walking device. *Nano Lett.* **4**, 1203–1207 (2004).
7. Shin, J. S. & Pierce, N. A. A synthetic DNA walker for molecular transport. *J. Am. Chem. Soc.* **126**, 10834–10835 (2004).
8. Bath, J., Green, S. J. & Turberfield, A. J. A free-running DNA motor powered by a nicking enzyme. *Angew. Chem. Int. Ed.* **44**, 4358–4361 (2005).
9. Tian, Y., He, Y., Chen, Y., Yin, P. & Mao, C. D. A DNzyme that walks processively and autonomously along a one-dimensional track. *Angew. Chem. Int. Ed.* **44**, 4355–4358 (2005).
10. Yin, P., Choi, H. M. T., Calvert, C. R. & Pierce, N. A. Programming biomolecular self-assembly pathways. *Nature* **451**, 318–322 (2008).
11. Omabegho, T., Sha, R. & Seeman, N. C. A Bipedal DNA Brownian motor with coordinated legs. *Science* **324**, 67–71 (2009).
12. Pei, R. et al. Behavior of polycatalytic assemblies in a substrate-displaying matrix. *J. Am. Chem. Soc.* **128**, 12693–12699 (2006).
13. Rothemund, P. W. K. Folding DNA to create nanoscale shapes and patterns. *Nature* **440**, 297–302 (2006).
14. Bonabeau, E., Dorigo, M. & Theraulaz, G. *Swarm Intelligence: From Natural to Artificial Systems* (Oxford Univ. Press, 1999).
15. Rus, D., Butler, Z., Kotay, K. & Vona, M. Self-reconfiguring robots. *Commun. ACM* **45**, 39–45 (2002).
16. Von Neumann, J. *Theory of Self-Reproducing Automata* (ed. Burks, A. W.) (Univ. Illinois Press, 1966).
17. Bennett, C. H. The thermodynamics of computation—a review. *Int. J. Theor. Phys.* **21**, 905–940 (1982).
18. Santoro, S. W. & Joyce, G. F. A general purpose RNA-cleaving DNA enzyme. *Proc. Natl Acad. Sci. USA* **94**, 4262–4266 (1997).
19. Antal, T. & Krapivsky, P. L. Molecular spiders with memory. *Phys. Rev. E* **76**, 021121 (2007).
20. Saffarian, S., Collier, I. E., Marmor, B. L., Elson, E. L. & Goldberg, G. Interstitial collagenase is a Brownian ratchet driven by proteolysis of collagen. *Science* **306**, 108–111 (2004).
21. Ke, Y., Lindsay, S., Chang, Y., Liu, Y. & Yan, H. Self-assembled water-soluble nucleic acid probe tiles for label-free RNA hybridization assays. *Science* **319**, 180–183 (2008).
22. Yurke, B., Turberfield, A. J., Mills, A. P., Simmel, F. C. & Neumann, J. L. A DNA-fuelled molecular machine made of DNA. *Nature* **406**, 605–608 (2000).
23. Li, J., Zheng, W., Kwon, A. H. & Lu, Y. *In vitro* selection and characterization of a highly efficient Zn(II)-dependent RNA-cleaving deoxyribozyme. *Nucleic Acids Res.* **28**, 481–488 (2000).
24. Walter, N. G., Huang, C.-Y., Manzo, A. J. & Sobhy, M. A. Do-it-yourself guide: how to use the modern single-molecule toolkit. *Nature Methods* **5**, 475–489 (2008).
25. Churchman, L. S., Ökten, Z., Rock, R. S., Dawson, J. F. & Spudich, J. A. Single molecule high-resolution colocalization of Cy3 and Cy5 attached to macromolecules measures intramolecular distances through time. *Proc. Natl Acad. Sci. USA* **102**, 1419–1423 (2005).
26. Yildiz, A. & Selvin, P. R. Fluorescence imaging with one nanometer accuracy: application to molecular motors. *Acc. Chem. Res.* **38**, 574–582 (2005).
27. Hess, H. Toward devices powered by biomolecular motors. *Science* **312**, 860–861 (2006).
28. Adleman, L. M. Molecular computation of solutions to combinatorial problems. *Science* **266**, 1021–1024 (1994).
29. Stojanovic, M. N. & Stefanovic, D. A deoxyribozyme-based molecular automaton. *Nature Biotechnol.* **21**, 1069–1074 (2003).
30. Seelig, G., Soloveichik, D., Zhang, D. Y. & Winfree, E. Enzyme-free nucleic acid logic circuits. *Science* **314**, 1585–1588 (2006).

Supplementary Information is linked to the online version of the paper at www.nature.com/nature.

Acknowledgements This research was supported by the US National Science Foundation (NSF) EMT and CBC grants (all authors); fellowships and grants from the Kinship Foundation (Searle), the Leukemia & Lymphoma Society, the Juvenile

Diabetes Research Foundation and NSF ITR (M.N.S.); awards from the US Army Research Office, the NSF, the US Office of Naval Research, the US National Institutes of Health, the US Department of Energy and a Sloan Research Fellowship (H.Y.); an NSF Graduate Fellowship (N.D.); and Molecular Biophysics and Microfluidics in Biomedical Sciences Training Fellowships from the NIH (A.J.-B. and N.M., respectively). M.N.S. is grateful to T. E. Mitchell and M. Olah for inspiration, discussions and help.

Author Contributions AFM experiments were performed by K.L. (majority), J.N. and N.D.; analysis was performed by N.D., K.L., J.N. and S.T. and supervised by E.W. and H.Y. Fluorescence microscopy and particle tracking analysis were performed

by A.J.M., N.M. and A.J.-B, supervised by N.G.W. Spiders were synthesized and purified, and their integrity was confirmed and monitored, by S.T. Surface plasmon resonance experiments were performed by R.P. Research coordination was by M.N.S. and materials transfer coordination was by S.T., J.N. and K.L. Experimental design and manuscript preparation received input from all authors.

Author Information Reprints and permissions information is available at www.nature.com/reprints. The authors declare no competing financial interests. Correspondence and requests for materials should be addressed to M.N.S. (mns18@columbia.edu), N.G.W. (nwalter@umich.edu), E.W. (winfree@caltech.edu) or H.Y. (hao.yan@asu.edu).